Chromium improvements on the mechanical performance of a rapidly solidified eutectic Sn–Ag alloy

Mohammed S. Gumaan[1]

Abstract

The eutectic Sn–Ag alloy considered a good replacement to the conventional solders. This study aims to enhance the mechanical performance of the eutectic Sn–Ag alloy in terms of both elasticity and plasticity through investigating the effects of chromium (Cr) content with $x = 1$, 3, and 5 wt.% on the mechanical and thermal properties of melt-spun Sn–3.5%Ag alloy. Ternary melt-spun Sn–Ag–Cr alloys investigated using x-ray diffractions (XRD), Scanning electron microscope (SEM), Instron machine, Vickers hardness tester, and Differential scanning calorimetry (DSC). The results revealed that the Cr content modifies the microstructure by refining the microstructure of the matrix of Sn solder; suppressing coarse inter-metallic compound (IMC) formation; and changing the morphology of the IMC in Sn solder. The high concentration of multi-oriental Ag_3Sn that formed with 3 wt.% of Cr, in addition to the compatibility among β-Sn (Tetragonal), Ag_3Sn (004) (orthorhombic), and Cr (200) (bcc), enhance the elasticity of melt-spun $Sn_{93.5}$–$Ag_{3.5}$–Cr_3 solder alloy by 330% (87.98 GPa) and obstructed the fracture process. The tensile test for that melt-spun alloy (3 wt.% of Cr) showed obvious improvements in ultimate tensile strength (UST) by 19% (23.42 MPa), and in toughness by 15.31% (911.15 J m^{-3}) compared to that of the eutectic melt-spun Sn–Ag alloy. Its hardness (Vickers hardness) value has improved by 22.37% (171.50 GPa) compared with that of the eutectic melt-spun Sn–Ag alloy. Slight improvements in thermal performance for that alloy have appeared through thermal conductivity by 8% (49.971 w m^{-1} k^{-1}) and thermal diffusivity by 85.4% (2.758×10^{-7} m^2 s^{-1}) compared to that of the eutectic melt-spun Sn–Ag alloy. All of the above-mentioned improvements are related to the microstructural changes with 3 wt.% of Cr to the eutectic Sn–Ag alloy. The high elasticity, high plasticity, low ΔT, and relatively low melting temperature (T_m) that have been taking place with 3 wt.% of Cr are suggested to increase the mechanical reliability of this alloy to become more desirable in soldering applications and electronic assembly.

1 Introduction

One of the most important parts of soldering technology is a solder alloy that is used to join the electronic devices to each other. The eutectic Sn–Ag alloy is one of the eco-friendly and popular alloys that have been used to achieve mechanical, electrical, and thermal connections among the electronic circuits. As long as the plasticity (ultimate tensile strength (UTS) + toughness) and elasticity (as modulus of elasticity (E) or Young's modulus) of any soldering material represents the core of its mechanical performance, many attempts have been done to improve the mechanical performance of

the eutectic Sn–Ag alloy [1–3]. But more studies are still required to enhance the performance of solder alloys in terms of mechanical and thermal connecting.

Also, the solidification technique (way) plays a vital role in influencing the microstructure guiding to improve the quality of the products. So, the solder's composition and solidification methods have great effects on the mechanical and thermal properties of the solder alloys, thus enhancing the quality of a solder alloy [4]. The effects of Ag content and Ni additions on the microstructures of Sn–Ag solders, thus tensile results have been reported by F.X. Che et. al [5]. They have concluded that the elastic modulus, yield stress, and UTS increase with increasing Ag content, and the solder alloys with high Ag content exhibit high strength due to the high concentration of IMC precipitates and fine Sn dendrites. Nevertheless, the elongation at UTS and elongation at fracture have been decreased with increasing Ag content; they treated those

✉ Mohammed S. Gumaan
    m.gumaan1@gmail.com

[1] Biomedical Engineering Department, Faculty
    of Engineering, University of Science & Technology, Sana'a,
    Yemen

problems by some Ni additives to enhance the ductility of that solder alloy. So, in the present work, it has been decided to fix the Ag content at the eutectic weight percent (3.5 wt.%) to avoid the reduction in elastic modulus and elongation at fracture. Huan Wang et. al [6] have reported significant improvement in the oxidation resistance of an Sn–3Ag–3Bi alloy with some small additions of Cr, this improvement was due to the refined microstructures with Cr additions. Guobiao Su et. al [7] investigated the 0.05% Cr effect on the growth of the intermetallic compound (IMC) layer for the Sn–Ag–Cu lead-free solder joint during isothermal aging. They revealed that the Cr content reduces the thickness of a layer of IMC as Sn–3.0Ag–0.3Cu–0.05Cr/Cu substrate during isothermal aging. By more research, and to best of our knowledge it can be said, there is a lake in research that interests both elasticity and plasticity of the eutectic Sn–Ag alloy. Therefore, the present work aims to improve both elasticity and plasticity of the eutectic Sn–Ag alloy, guiding it to be more reliable in the electronic assembly applications. By continuing the previous work [8] (small additions of Cr < 1 wt.%), and to achieve the above-mentioned aim, this study will investigate the effects of Cr content (medium additions > 1 wt.%) on the microstructural, mechanical, and thermal properties of Sn–3.5Ag solder. This work concentrates on the effects of phase orientation of Ag_3Sn and its concentration on the aforementioned physical properties of Sn–Ag–Cr solders.

2 Experimental procedure

2.1 Materials preparation

Three different concentrations of chromium (Cr) content (as 1, 3, and 5 wt.%) were selected as reinforcement additions to the eutectic melt-spun Sn–Ag alloy. The purity of all elements Sn, Ag, and Cr is about 99.9%. The four alloy systems studied (Sn–3.5Ag–xCr where $x = 1$, 3, and 5) were solidified rapidly, utilizing a smoothly singular roll of melt-spinning technique. These four alloy systems were prepared through heating them, using electric furnace to the liquid state. They were manually agitated at approximately 80 °C above their melting points to achieve homogenization. Then putting them again inside an electric furnace for 25 min, the molten alloy systems were poured down the surface of a highly rotating, with a velocity approximately equal to 31.5 m/s, copper roll of the melt-spinning technique. The producing alloy systems had long strips form, with the 50–70 μm thickness and 5 mm width. After that, and using a double knife cutter, the strips were cut into ribbons in suitable shapes [9].

2.2 Materials investigation

X-ray diffractometer with CuKa radiation ($\lambda = 0.15406$ nm) was used for XRD measurements. XRD patterns were recorded within the 2θ vary of 20°–90°. The elastic modulus (modulus of elasticity E) determinations were implemented by tensile strength (TS). The tensile tests were performed using a computerized locally made tensile test machine. Every specimen was stretched until the fracture under the effect of 0.5 mm/min strain rate and room temperature [10]. The morphological microstructure of four alloy systems after polishing was observed using a scanning electron microscope (SEM) (JEOL, JSM-5400). The thermal parameters were determined by the utilization of the differential scanning calorimetry (DSC) Shimadzu DSC-50. The measurements were performed at a heating rate of 10 °C/min and high-purity chemical element gas taste heating chamber to avoid oxidization of samples. The Vickers microhardness numbers (H_V) were measured using the FM-7 microhardness tester at 25-g force (gf) load for 5 s as shown in the previous work [11].

3 Results and discussion

3.1 Structural analysis

The x-ray diffraction (XRD) patterns for melt-spun Sn–3.5Ag–xCr solders with $x = 0$, 1, 3, and 5, respectively, have been shown in Fig. 1. Sn–3.5Ag solder exhibits two peaks for Ag_3Sn despised in Sn matrix as shown in SEM images Fig. 2 and presented in the previous work [12]. Adding 1 wt.% of Cr does alter the Ag_3Sn (012) and Ag_3Sn
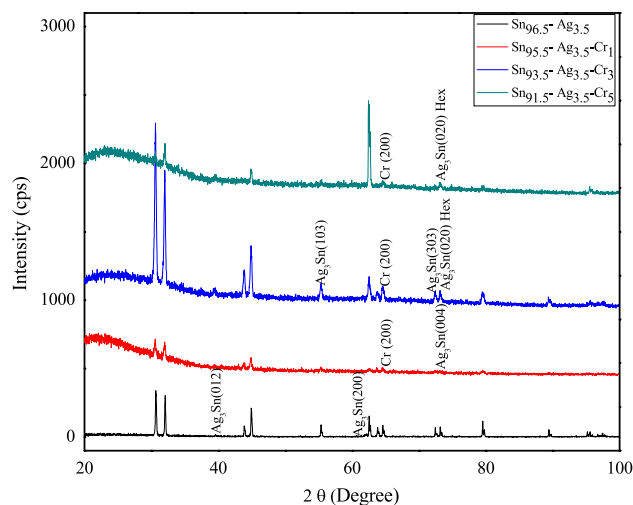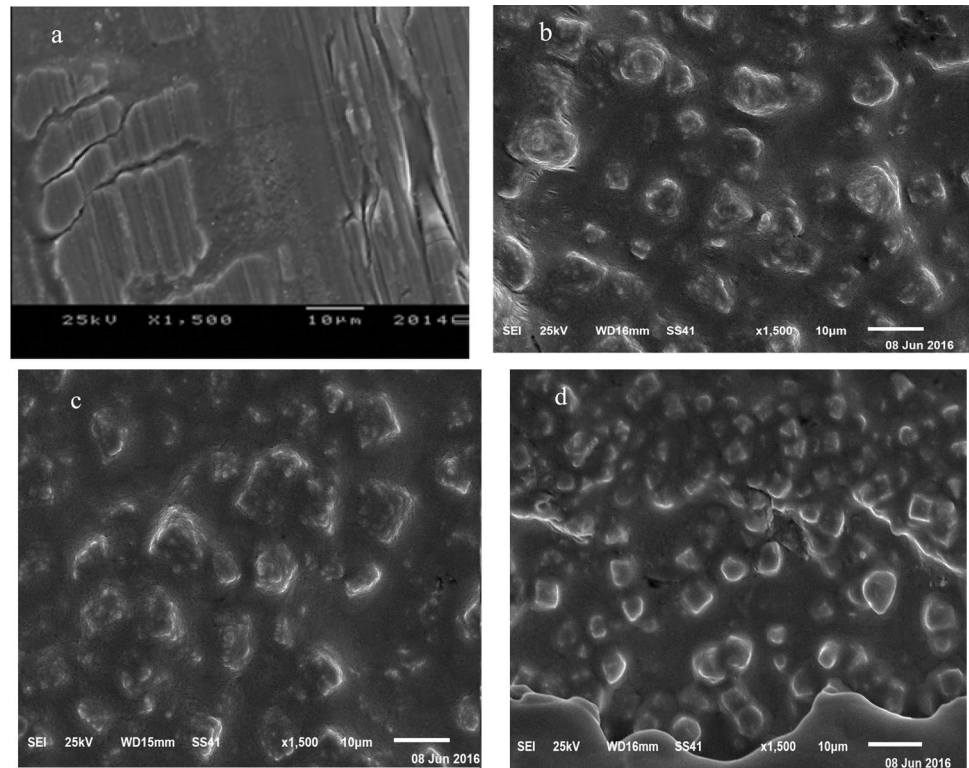

Fig.1 The XRD patterns of the melt-spun Sn–Ag–Cr solders

Fig. 2 SEM images of the melt-spun **a** Eutectic Sn–Ag, **b** $Sn_{95.5}$–$Ag_{3.5}$–Cr_1, **c** $Sn_{93.5}$–$Ag_{3.5}$–Cr_3, and **d** $Sn_{91.5}$–$Ag_{3.5}$–Cr_5 solder alloys

(200) peaks to the Ag_3Sn (004) one, there was one peak corresponding to the Cr phase. Cr was not observed in the Ag_3Sn IMC phase, and Cr did not form IMCs in the solidification reactions. This result indicates a partial dissolving of Cr content inside Sn matrix and undissolved Cr atoms have precipitated as Cr phase. The particle sizes of β-Sn and Ag_3Sn for all melt-spun Sn–3.5Ag–xCr solders were calculated using Scherrer Formula [13]: $t = (0.9\,\lambda/B\,\cos\theta_B)$, where B is the broadening of diffraction line measured at half of its maximum intensity (radians), t is the diameter of crystal particle, θ_B is the Bragg angle, and λ is the wavelength of x-ray. The above-mentioned addition (1 wt.% of Cr) of Cr refines the sizes of Sn and Ag_3Sn, where the Cr atoms work to prevent Sn and Ag_3Sn growth through the solidification process. This addition (1 wt.% of Cr) of Cr also changes the Ag_3Sn orientation from (012, and 200) to (004). A lattice strain value of the eutectic Sn–Ag alloy (7.56×10^{-4}) has been increased to (12.19×10^{-4}) with that addition. This increment is due to particle size reduction according to G. K. Williamson and W. H. Hall [14]:

$$B = \left(\frac{1}{D_{eff}}\right) + 5\ \leq \varepsilon^2 \geq^{1/2} \sin\frac{\theta}{\lambda}, \qquad (1)$$

where D_{eff} `D_{eff} is the crystallite size, and ε is local lattice distortion in the β-Sn matrix.

A slight change has been occurred in (c/a) values from (0.545) to (0.542) due to a lattice expanding in a-axis and contracting in c-axis with 1 wt.% of Cr and it also decreased with the other Cr additions. This distortion reduces the number of atoms per unit cell (N), which indicates the lattice point defects. With 3 wt.% of Cr, the particle size of β-Sn has been decreased to (33.07 nm), this decrement is due to the fact that the Cr atoms worked as barriers for the growth of Sn crystals through the solidification process. Cr atoms pushed the Ag atoms to strongly interact with β-Sn to build more Ag_3Sn phases with different orientations (Fig. 1) and bigger size (43.18 nm) as shown in Table 1. The evidence of happening the above-mentioned mechanism is the same precipitations from Cr inside the β-Sn matrix. With Cr additions, the c/a values have been decreased due to a-axis expanding, which leads to increase in the cell volumes of these alloy systems. This expanding leads to the reduction in the number of atoms per unit cell, thus more point defects. With the addition of 5 wt.% of Cr, the particle size of β-Sn has increased (55.39 nm), whereas the Ag_3Sn concentration (one peak Fig. 1) and size (43.41 nm) have been reduced. This may attribute to the limited solubility of Cr in β-Sn. These changes may be because those Cr atoms work as a closed area to prevent Ag from interacting with Sn matrix. The increased particle size reduces the lattice distortion ε (12×10^{-4}). Ag_3Sn (103 and 303) have been disappeared with 5 wt.% of Cr. The details of the XRD analysis are shown in Table 1.

Table 1 The lattice parameters and XRD details

Alloy	Particle size of β-Sn phase (nm)	Particle size of Ag$_3$Sn phase (nm)	Lattice strain (ε)$\times 10^{-4}$	c (Å)	a (Å)	c/a	Cell volume (Å)^3	Number of atoms per unit cell of tin phase (N)
Eutectic Sn–Ag	71.89	98.41	7.56	3.307	5.83	0.545	108.1789	3.182
Sn$_{95.5}$–Ag$_{3.5}$–Cr$_1$	55.71	10.15	12.19	3.167	5.835	0.542	107.8666	2.944
Sn$_{93.5}$–Ag$_{3.5}$–Cr$_3$	33.07	43.18	14.41	3.108	5.992	0.518	111.6285	2.54
Sn$_{91.5}$–Ag$_{3.5}$–Cr$_5$	55.39	43.41	12.2	3.023	6.15	0.491	114.3797	2.309

3.2 Microstructure

According to the SEM analysis results shown in Fig. 2a, two different solid phases (black and white lamellar) grew at the Sn–Ag eutectic alloy. The black phase is β-Sn and the white lamellar phase is Ag$_3$Sn intermetallic. When 1 wt.% of Cr Fig. 2b is added to the eutectic alloy, two different solid phases (black and white) have appeared. The black is β-Sn and the white phase is Ag$_3$Sn intermetallic. In Fig. 2c, the particle size of β-Sn (black) refined as confirmed in XRD data. Also, more ductile morphology is occurred containing three different solid phases (black, dark gray, and white), these phases are supposed to be β-Sn, Cr, and Ag$_3$Sn, respectively. The black, dark gray, and white regions appeared in Fig. 2d, where the refined particle size of Ag$_3$Sn occurred. These features are strongly related with the crystallite sizes in Table 1, while the microstructure of Sn–3.5Ag–xCr alloys, which is the dispersed particle of Ag$_3$Sn-rich phase in the β-Sn matrix, is much finer and uniform, there is little difference in the microstructure of different Cr content. Generally, it was observed that the Cr content modifies the microstructure, by refining the microstructure of the Sn-solder matrix; suppressing coarse intermetallic compound (IMC) formation; and changing the morphology of the IMC in Sn solder.

3.3 Mechanical properties

Based on the XRD data, the concentration and orientation of Ag$_3$Sn IMC that is finely dispersed in Sn matrix are affected by Cr content. In addition, and to supply reliable mechanical performance, which is originally related to the stability in microstructure with respect to traditional solders, elastic modulus (E) is highly important. Its importance arises from its ability to estimate the bonding nature among constituent atoms [15–17]. Table 2 shows some mechanical parameters for all the melt-spun alloys like E which is calculated according to the following equation [18]:

$$E = 38.32 \left[\rho L^4 f^2 / t^2 \right], \tag{2}$$

where ρ is the density, L is the length of the ribbon, f is the resonance frequency, and t is the ribbon thickness.

By adding 1 wt.% of Cr, the increase in elastic modulus (E) is about 330% (87.98 GPa). Since Young's modulus (E) is the only one that is relatively sensitive to microstructures and is primarily determined by the chemical bonding among atoms, the other mechanical properties are all sensitively influenced by microstructures (alloying elements and alloy processing). The change in orientation of Ag$_3$Sn from (012, and 200) to (004) and precipitating Cr (200) as shown in Fig. 1 led to the increment in elastic modulus (E). The reason for that may be due to the compatibility among β-Sn (Tetragonal), Ag$_3$Sn (004) (orthorhombic), and Cr (200) (bcc). Increasing Young's modulus (E) means an atomic bond increasing, which is basically dependent on the crystal structure type and atomic package [19]. The values of Young's modulus (E) continued varying with Cr additions due to the reduction of particle size of β-Sn as shown in XRD data. As well known, the ultimate tensile strength (UTS) is primarily influenced by the microstructure (alloying elements and alloy processing). So, and as occurred in Fig. 3 (stress–strain curves) and Table 2, the values of UTS have been increased with Cr additions. The highest value of UTS has occurred with 1 wt.% of Cr to the eutectic Sn–Ag alloy. The reason may is the lake of orientation's diversity of IMC's (Ag$_3$Sn (004)) and the solid solution strengthening of Cr content for Sn matrix. The solid solution strengthening

Table 2 Mechanical parameters

Alloy	E (GPa)	UTS (MPa)	Toughness (J m^{-3})	Density (g cm^{-3})	H_v (5 s) (MPa)
Eutectic Sn–Ag	20.42	19.66	790.16	6.005	140.14
Sn$_{95.5}$–Ag$_{3.5}$–Cr$_1$	38.81	33.7	266.7	6.361	136.71
Sn$_{93.5}$–Ag$_{3.5}$–Cr$_3$	87.98	23.42	911.15	6.469	171.5
Sn$_{91.5}$–Ag$_{3.5}$–Cr$_5$	74.82	28.7	316.6	5.966	159.25

Fig. 3 Stress–Strain curves of the melt-spun Sn–Ag–Cr solder alloys

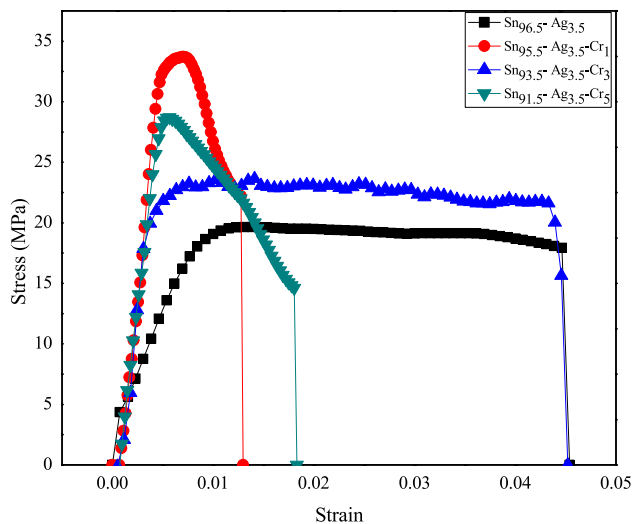**Fig.4** DSC curves of the melt-spun Sn–Ag–Cr solder alloys

may be more predictable with the low precipitators of Cr and IMCs phases. With a 3 wt.% of Cr, its UTS increased at a moderate level by 19% (23.42 MPa), but the plasticity of that alloy has been improved. The plasticity improvement has been noticed through the highest value of the toughness for that alloy (911.15 J m^{-3}); this means it has improved by 15.31% compared to that of the eutectic Sn–Ag alloy. The diversity of IMC's phase orientation which works as barriers for crack propagation may be the main cause to enhance the toughness of that alloy (3 wt.% of Cr). This explanation came from the principle which says that the diverse phase orientations may give chance to the lattice to be re-arranged instead of the fracture. This feature strongly benefits soldering and assembly applications where it works as a deformation alarm before fracture point instead of a dangerous brittle fracture. From the values of Young's modulus E (87.98 Gpa) and toughness (911.15 J m^{-3}) for that alloy with addition of 3wt.% of Cr, it can be said that the elasticity and plasticity of the eutectic Sn–Ag alloy have been improved. So, the Cr content (3 wt.% of Cr) increased the elasticity (Young's modulus (E)), ultimate tensile strength (UTS), and plasticity [toughness (911.15 J m^{-3})] and promoted the ductile fracture. With the other Cr additions, the elasticity and plasticity of the solders decreased and brittle fracture modes were seen. The Vickers hardness results calculated according to the following equation [20]:

$$H_v = \frac{1.854\ F}{L^2},\tag{3}$$

where F is the applied load (measured in kilograms-force) and L^2 the area of the indentation (measured in square millimeters) showed an improvement (increment) by 22.37% (171.50 GPa) compared to that of the eutectic Sn–Ag alloy as shown in Table 2. The high hardness number of that
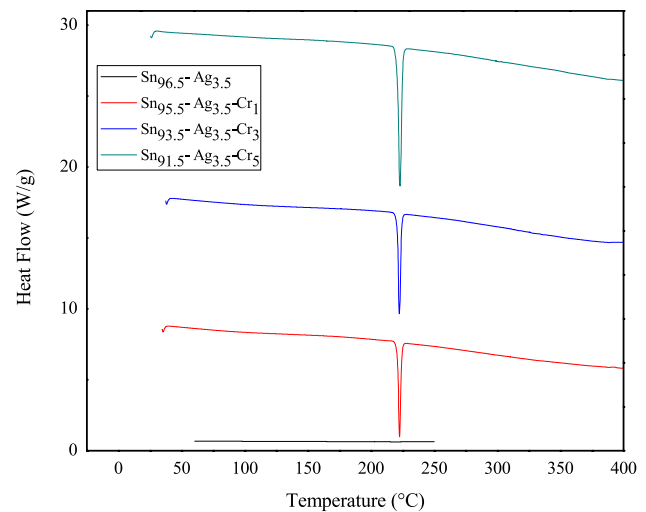
solder alloy with 3 wt.% of Cr addition attributes to the high possibility for indentor to be on Cr and/or Ag$_3$Sn precipitates embedded in the Sn matrix as explained XRD and shown in SEM.

3.4 Thermal and electrical behavior

The thermal performance of the obtained melt-spun Sn–Ag–Cr alloy systems were accurately characterized by DSC thermograms as shown in Fig. 4. The range of test temperature was from 30 to 400 °C and heating rate 10 °C min^{-1}. The thermal performance of the solder materials is so important in electronic devices and their applications. This importance has raised from the thermal vital role of a solder alloy as a thermal connector inside the electronic circuits. The first desirable thermal property of a solder joint is to be low processing temperature and high working temperature, this feature makes the solder joint easier in a needed shape and thermally reliable to serve at elevated temperatures, respectively [21]. The second desirable one is a thermal conductivity, which is a crucial property for the reliability and the lifespan of power devices since the operation requires continuous heat dissipation during service. These desirable features are strongly related to the material's composition and microstructure of a solder material. As shown in Table 3, the melting temperatures (T_m) of the melt-spun Sn–Ag–Cr solder alloys have been increased, (approximately ≈ 222.46 °C) compared to the melting temperature of the eutectic Sn–Ag alloy. The reason may be the presence of Cr phase, which is originally a high melting temperature's phase. The needed energies by the melt-spun Sn–Ag–Cr alloys to be in a liquid state (enthalpy ΔH) are higher than that of the eutectic Sn–Ag alloy. It may be due to the thermal nature of a precipitated Cr phase, as shown in XRD. With

Table 3 Thermal parameters

Alloy	T_m (°C)	ΔH (j/g)	C_p (j/g.k)	ΔT (°C)	Thermal conductivity (w m^{-1} k^{-1})	Thermal diffusivity $\times 10^{-7}$ (m^2 s^{-1})
Eutectic Sn–Ag	217.4	1.391	0.067	6.05	46.262	1.487
$Sn_{95.5}$–$Ag_{3.5}$–Cr_1	222.65	42.03	2.643	15.9	38.498	0.594
$Sn_{93.5}$–$Ag_{3.5}$–Cr_3	222.46	45.16	3.716	12.15	49.971	2.758
$Sn_{91.5}$–$Ag_{3.5}$–Cr_5	222.98	56.5	4.498	12.86	28.85	0.893
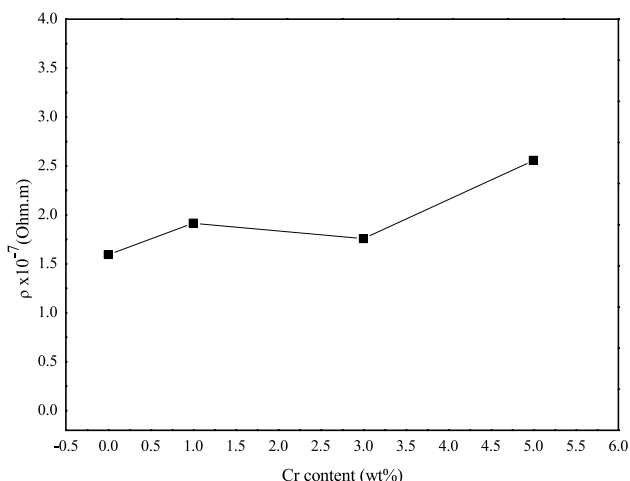
Fig.5 Electrical resistivity versus Cr content of the melt-spun Sn–Ag–Cr solder alloys

Cr additions, the specific heat capacities (c_p) have increased, thus the values of the thermal conductivities are expected to be increased. This is because the thermal conductivity of any solder alloy is determined by thermal diffusion coefficient, density, and specific heat capacity, as given by the following equation [21]:

$$k = \alpha \rho c_p. \tag{4}$$

The thermal conductivities of melt-spun Sn–Ag–Cr alloys have improved by 8% (49.971 w m^{-1} k^{-1}) as shown in Table 3. One of the privileges of the melt-spinning technique is to reduce the time needed of any alloy to be completely solidified compared with the conventional techniques. This means low pasty range ΔT achieved where the high pasty range leads to more cracks and micro-segregation in the soldering process [22]. 3 wt.% of Cr addition has the lowest pasty range among all other additions. 3 wt.% of Cr addition has the best thermal behaviour, and the mechanical competition revealed that it has a clear superiority in comparison with the other additions so, its performance makes it a favorable candidate for solder applications. Figure 5 shows that the $Sn_{93.5}$–$Ag_{3.5}$–Cr_3 melt-spun solder alloy has the lowest electrical resistivity (highest electrical conductivity)

compared with the other alloy systems. These mechanical enhancements, good electrical behavior besides the reasonable (suitable) thermal performance increase the reliability of this alloy to be more desirable in the electronic applications.

4 Conclusions

To adequately enhance the mechanical and electrical performance of a melt-spun Sn–3.5Ag solder alloy for electronic applications with respect to acceptable (suitable) thermal properties, in terms of both elasticity with plasticity, thermal conductivity, and electrical conductivity, which are basically related to the microstructures of the solder alloys, the chromium (Cr) effects on the eutectic Sn–Ag alloys have been investigated. In addition to the high concentration of multi-oriental Ag_3Sn, the compatibility among β-Sn (Tetragonal), Ag_3Sn (004) (orthorhombic), and Cr (200) (bcc) enhances the elasticity of melt-spun $Sn_{93.5}$–$Ag_{3.5}$–Cr_3 solder alloy by 330% (87.98 GPa). The plasticity of that solder alloy is also improved through the toughness by 15.31% (911.15 J m^{-3}), and ultimate tensile strength (UST) by 19% (23.42 Mpa) compared with that of the eutectic melt-spun Sn–Ag alloy. It has been observed that a 3 wt.% of Cr addition to the eutectic melt-spun Sn–Ag alloy, increased its Vickers hardness about 22.37% (171.50 GPa). Finally, the improvement in thermal performance of that alloy was appeared through thermal conductivity by 8% (49.971 w m^{-1} k^{-1}) and thermal diffusivity by 85.4% (2.758$\times 10^{-7}$ m^2 s^{-1}) compared to that of the eutectic Sn–Ag alloy. The above-mentioned improvements are attributed to the microstructural changes with 3 wt.% of Cr doped to the eutectic Sn–Ag alloy. The high elasticity, high plasticity, low ΔT, and relatively low T_m that have been taken place with 3 wt.% of Cr are suggested to increase the mechanical reliability of this alloy to become more desirable in the soldering applications and electronic assembly.

References

1. S.A.C. Al, S.M. Technology, V. Iss, M.O. Components, J.H. Vincent, H.A.H. Steen, Lead-free reflow soldering for electronics assembly. Solder. Surf. Mt. Technol. **13**, 21–38 (2001)
2. M.S. Gumaan, R.M. Shalaby, E.A.M. Ali, M. Kamal, Copper effects in mechanical, thermal and electrical properties of rapidly

solidified eutectic Sn–Ag alloy. J. Mater. Sci. Mater. Electron. **29**, 8886–8894 (2018)

3. E.A.M. Shalaby, R.M. Kamal, M. Ali et al., Design and properties of new lead-free solder joints using Sn-3.5Ag-Cu solder. Silicon. **10**, 1861–1871 (2018)

4. P.J.A. Verma, S.P. Tewari, Vibratory stress, solidification and microstructure of weldments under vibratory welding condition—A review, Int. J. Eng. Sci. Technol. 3 (2011) 5215–5220. https://www.scribd.com/document/332150758/VIBRATORY-STRESS-SOLIDIFICATION-AND-MICROSTRUCTURE-OF-WELDMENTS-UNDER-VIBRATORY-WELDING-CONDITION-A-REVIEW-pdf. Accessed June 26, 2019

5. X.R.Z.F.X. Che, W.H. Zhu, E.S.W. Poh, X.W. Zhang, The study of mechanical properties of Sn-Ag-Cu lead-free solders with different Ag contents and Ni doping under different strain rates and temperatures. J. Alloys Compd. **507**, 215–224 (2010)

6. H. Wang, A. Hu, C. Chang, M. Li, D. Mao, Oxidation behavior and intermetallic compounds growth of Sn-Ag-Bi-Cr lead-free solder, *Proceedings of Electronic Packaging Technology Conference EPTC* (Piscataway, IEEE, 2007)

7. G. Su, Y. Han, C. Wang, H. Wang, X. Wei, Effect of 0.05% Cr on intermetallic compound layer growth for Sn-Ag-Cu lead-free solder joint during isothermal aging, *Proceedings of the International Symposium on Physical and Failure Analysis of Integred Circuits* (IPFA, London, 2009), pp. 393–396

8. S.R. Abbas, M.S. Gumaan, R.M. Shalaby, Chromium effects on the microstructural, mechanical and thermal properties of a rapidly solidified eutectic Sn-Ag alloy. Solder. Surf. Mt. Technol. **32**, 137–145 (2019)

9. M. Kamal, U. Mohammad, *A review: chill-block melt spin technique, theories & applications* (Bentham Science Publishers, Sharjah, 2012)

10. G. Saad, S.A. Fayek, A. Fawzy, H.N. Soliman, G. Mohammed, Deformation characteristics of Al-4043 alloy. Mater. Sci. Eng. A. **527**, 904–910 (2010)

11. M.M. Jubair, M.S. Gumaan, R.M. Shalaby, Reliable Sn-Ag-Cu lead-free melt-spun material required for high-performance applications. Zeitschrift Fur Krist. - Cryst. Mater. **234**, 757–767 (2019)

12. R.M. Shalaby, M. Kamal, E.A.M. Ali, M.S. Gumaan, Microstructural and mechanical characterization of melt spun process Sn-3.5Ag and Sn-3.5Ag-xCu lead-free solders for low cost electronic assembly. Mater. Sci. Eng. A. **690**, 446–452 (2017)

13. B.D. Cullity, *Elements of X-ray diffraction* (Reading, Addison-Wesely, 1978), p. 248

14. G. Williamson, W. Hall, X-ray line broadening from filed aluminium and wolfram. Acta Metall. **1**, 22–31 (1953)

15. A. Inoue, H.S. Chen, J.T. Krause, T. Masumoto, M. Hagiwara, Young's modulus of Fe-, Co-, Pd- and Pt-based amorphous wires produced by the in-rotating-water spinning method. J. Mater. Sci. **18**, 2743–2751 (1983)

16. A.M. Hezma, I.S. Elashmawi, E.M. Abdelrazek, A. Rajeh, M. Kamal, Enhancement of the thermal and mechanical properties of polyurethane/polyvinyl chloride blend by loading single walled carbon nanotubes. Prog. Nat. Sci. Mater. Int. **27**, 338–343 (2017)

17. M.M. Abutalib, A. Rajeh, Influence of MWCNTs/Li-doped TiO_2 nanoparticles on the structural, thermal, electrical and mechanical properties of poly (ethylene oxide)/poly (methylmethacrylate) composite. J. Organomet. Chem. **918**, 121309 (2020)

18. M.S. Gumaan, R.M. Shalaby, M.K. Mohammed Yousef, E.A.M. Ali, E.E. Abdel-Hady, Nickel effects on the structural and some physical properties of the eutectic Sn-Ag lead-free solder alloy. Solder. Surf. Mt. Technol. **31**, 40–51 (2019)

19. Y.L. Zhou, M. Niinomi, T. Akahori, Effects of Ta content on Young's modulus and tensile properties of binary Ti-Ta alloys for biomedical applications. Mater. Sci. Eng. A. **371**, 283–290 (2004)

20. T. El-Ashram, R.M. Shalaby, Effect of rapid solidification and small additions of Zn and Bi on the structure and properties of Sn-Cu eutectic alloy. J. Electron. Mater. **34**, 212–215 (2005)

21. C. Hang, J. He, Z. Zhang, H. Chen, M. Li, Low temperature bonding by infiltrating Sn3.5Ag solder into porous Ag sheet for high temperature die attachment in power device packaging. Sci. Rep. **8**, 2–8 (2018)

22. R.M. Shalaby, Effect of silver and indium addition on mechanical properties and indentation creep behavior of rapidly solidified Bi-Sn based lead-free solder alloys. Mater. Sci. Eng. A. **560**, 86–95 (2013)